Published in final edited form as:
Neuropharmacology. 2014 February ; 77: . doi:10.1016/j.neuropharm.2013.09.023.

[^{125}I]AT-1012, a New High Affinity Radioligand for the α3β4 Nicotinic Acetylcholine Receptors

Jinhua Wu[a], **David C. Perry**[b], **James E. Bupp**[c], **Faming Jiang**[d], **Willma E. Polgar**[c], **Lawrence Toll**[a], and **Nurulain T. Zaveri**[d]

[a]Torrey Pines Institute for Molecular Studies, 11350 SW Village Parkway, Port St. Lucie, FL 34987, USA

[b]Department of Pharmacology & Physiology, George Washington University, 2300 Eye St NW, Washington DC, 20037, USA

[c]SRI International, 333 Ravenswood Ave., Menlo Park, CA 94025, USA

[d]Astraea Therapeutics, 320 Logue Avenue, Suite 142, Mountain View, CA 94043, USA

Abstract

Recent genetic and pharmacological studies have implicated the α3, β4 and a5 subunits of the nicotinic acetylcholine receptor (nAChR) in dependence to nicotine and other abused drugs and nicotine withdrawal. The α3β4* nAChR subtype has been shown to co-assemble with the α5 or β3 nAChR subunits, and is found mainly in the autonomic ganglia and select brain regions. It has been difficult to study the α3β4 nAChR because there have been no selective nonpeptidic ligands available to independently examine its pharmacology. We recently reported the synthesis of a [^{125}I]-radiolabeled analog of a high affinity, selective small-molecule α3β4 nAChR ligand, AT-1012. We report here the vitro characterization of this radioligand in receptor binding and in vitro autoradiographic studies targeting the α3β4* nAChR. Binding of [^{125}I]AT-1012 was characterized at the rat α3β4- and α4β2 nAChR transfected into HEK cells as well as at the human α3β4α5 nAChR in HEK cells. Binding affinity of [^{125}I]AT-1012 at the rat α3β4 nAChR was 1.4 nM, with a Bmax of 10.3 pmol/mg protein, similar to what was determined using [^{3}H]epibatidine. Saturation isotherms suggested that [^{125}I]AT-1012 binds to a single site on the α3β4 nAChR. Similar high binding affinity was also observed for [^{125}I]AT-1012 at human α3β4α5 nAChR in a human α3β4aα nAChR transfected cell line. [^{125}I]AT-1012 did not bind with high affinity to membranes from α4β2 nAChR-transfected HEK cells, and [^{3}H]epibatidine binding studies showed that AT-1012 had over 100-fold binding selectivity for the α3β4 over α4β2 nAChR. K_i values determined for known nAChR compounds using [^{125}I]AT-1012 as radioligand were comparable to those obtained with [^{3}H]epibatidine. [^{125}I]AT-1012 was also used to label the α3β4 nAChR in rat brain slices in vitro using autoradiography which showed highly localized binding of the radioligand in brain regions consistent with the discreet localization of the α3β4 nAChR. We demonstrate that [^{125}I]AT-1012 is an excellent tool for labeling the α3β4 nAChR in the presence of other nAChR subtypes.

Corresponding Author: Dr. Nurulain Zaveri, Astraea Therapeutics, 320 Logue Avenue, Suite 142, Mountain View, CA 94043, USA. Tel: 650-254-0786, Fax: 650-254-0787, nurulain@astraeatherapeutics.com.

Statement of conflicts of interest

The authors declare that there are no conflicts of interest.

Keywords

Nicotinic acetylcholine receptor; alpha3beta4; AT-1012; receptor binding; in vitro autoradiography

1. Introduction

The α3β4* subtype of the nicotinic acetylcholine receptor (nAChR) is a minor component of the total complement of nAChRs in the brain. Historically, it has been more widely recognized as being present in the autonomic ganglia, and has been considered the ganglionic nAChR. In the brain, the α4β2* nAChR subtype is the predominant subtype, along with relatively high amounts of the homomeric α7 nAChR (Perry *et al*., 2002; Xiao *et al*., 2004). Although the α3β4* nAChR is present in relatively small amounts in the brain, it is very highly concentrated in a few brain regions. In particular, high concentrations of α3β4* nAChR are found in the medial habenula (MHb), the interpeduncular nucleus (IPN), and the fasciculus retroflexus (fr, the fiber tract that connects the MHb and IPN). Smaller amounts of α3β4* nAChR are also found in the pineal gland (Perry *et al*., 2002). The α3β4* nAChR have been shown to co-assemble with other nAChR subunits, mostly the α5 and the β3. The α5-containing α3β4* nAChR are predominantly found in the peripheral ganglia, whereas the α3β4 nAChR subpopulation in the IPN and MHb are predominantly associated with the β3 subunit, and to a much lesser extent with the α5 subunit (Gotti *et al*., 2009; Grady *et al*., 2009)). Although the α3β4* nAChR are not the predominant subtype in the brain, recent studies have suggested an important role of this nAChR subtype in drug dependence, particularly nicotine dependence. In experiments conducted on β4-null mice, precipitated withdrawal after chronic nicotine exposure was greatly reduced, suggesting the α3β4* nAChR activation is involved in development of withdrawal, one major factor leading to the difficulty in smoking cessation (Salas *et al*., 2004). In Genome Wide Association Studies (GWAS), variants in the CHRNA5/A3/B4 gene cluster on chromosome 15 have been associated with an increased risk of whether a smoker becomes nicotine-dependent, and to smoking a greater number of cigarettes per day (Berrettini *et al*., 2008; Saccone *et al*., 2008). Recent pharmacological studies also suggest that the α3β4 nAChR may be involved in the rewarding effects of nicotine, and possibly other drugs of abuse. We recently reported that AT-1001, a nanomolar affinity α3β4-selective nAChR antagonist blocks nicotine self-administration in rats at low doses, without non-specific effects on food responding (Toll *et al*., 2012). 18-methoxycoronaridine (18-MC), a derivative of the alkaloid ibogaine, has been shown to inhibit the rewarding effects of several abused drugs, including nicotine, cocaine, alcohol, morphine and methamphetamine through inhibition of α3β4* nAChR (Maisonneuve *et al*., 2003; Glick *et al*., 2000b; Glick *et al*., 2006; McCallum *et al*., 2009; Rezvani *et al*., 1997; Glick *et al*., 2002). However, 18-MC has been shown to have measurable affinity to other receptor sites, such as the opioid and 5-HT3 receptors (Glick *et al*., 2000a; Glick *et al*., 2000c), and therefore the involvement of other receptors contributing to 18-MC's mechanism of action cannot be ruled out.

With the emerging prominence of the α3β4* nAChR subtype in drug dependence, there is a need for developing 'selective' α3β4* nAChR ligands as tools to be able to study the pharmacology of this subtype, and its role as a possible target for drug abuse treatment. Although the α3β4 nAChR antagonist peptide α-conotoxin AuIB has been used to study the pharmacology of α3β4 nAChR in the brain (Grady *et al*., 2001; Luo *et al*., 1998; McCallum *et al*., 2012), this peptide requires direct injections into the brain and is not available as a radiolabeled analog for localization studies. Compounds like 18-MC and mecamylamine lack the high affinity and selectivity required in a useful tool to study the localization and pharmacology of this nAChR subtype, particularly given its limited distribution in the brain.

We recently reported the synthesis of a radioactive iodine-containing α3β4 nAChR ligand [^{125}I]AT-1012 (Jiang *et al*., 2012), which is an analog of the selective α3β4 nAChR ligand AT-1001 we reported earlier (Toll *et al*., 2012). As with AT-1001, AT-1012 has greater than 100-fold selectivity versus the α4β2 and α7 nAChR, in competition experiments with [^{3}H]-epibatidine. This radioligand can be a useful tool to study α3β4* nAChR distribution and pharmacology. Here we describe the detailed characterization of the binding profile of [^{125}I]AT-1012 and its utility as a radioligand for determining binding affinities of known and novel α3β4 nAChR ligands. We also report its binding to human α3β4α5-containing nAChR subpopulation in transfected cell lines. Further, we demonstrate its high selectivity for labeling the α3β4* nAChR population in rat brain using in vitro autoradiography.

2. Materials and Methods

2.1. Materials

[^{125}I]AT-1012 (Figure 1) was synthesized as previously described (Jiang *et al*., 2012). Additional AT compounds shown in Table 1 were synthesized in our laboratory by methods described in Jiang et al. (Jiang *et al*., 2012).

2.2. Cell Culture

KXα3β4R2 and KXα4β2R2 cells, containing rat α3β4 and α4β2 nAChR respectively (obtained from Drs. Kenneth Kellar and Yingxian Xiao, Georgetown University), were cultured in Dulbecco's modified Eagle's medium (DMEM), supplemented with 10% fetal bovine serum (FBS), 0.5% penicillin/streptomycin, and 0.4 mg/ml of geneticin, and were maintained in an atmosphere of 7.5% CO_2 in a humidified incubator at 37°C. For binding assays, cells were passaged on 150-mm dishes and harvested when confluent. Human α3β4a5 nAChR containing HEK cells were obtained from Dr. Jon Lindstrom (University of Pennsylvania). These cells were grown as discussed above except the growth medium contained 0.6 mg/ml geneticin, 0.5 mg/ml zeocin, and 0.2 mg/ml hygromycin.

2.3. Binding Assays

Cells were harvested by scraping the plates with a rubber policeman, suspended in 50 mM Tris buffer pH 7.4, homogenized using a Polytron Homogenizer, and the centrifugation was repeated twice at 20,000 × g (13,500 rpm) for 20 min. For binding, the cell membranes were incubated with the test compounds at concentrations generally ranging from 10^{-5} to 10^{-11} M in the presence of 0.03 nM [^{125}I]AT-1012 or 0.3 nM of [^{3}H]epibatidine. After 1 h of incubation, at room temperature, for [^{125}I]AT-1012 or 2 h for [^{3}H]epibatidine, samples were filtered, using a Tomtec cell harvester, through glass fiber filters that had been presoaked in 0.05% polyethyleneimine. Filters were counted on a betaplate reader (Wallac). Nonspecific binding was determined by using 1 μM of AT-1001 or 0.1 μM of unlabeled epibatidine. IC_{50} values and Hill coefficients were determined by using the program Graphpad/PRISM. K_i values were calculated using the Cheng Prusoff transformation: $K_i = IC_{50}/(1+L/K_d)$ (Cheng *et al*., 1973) where, L is radioligand concentration and K_d is the binding affinity of the radioligand, as determined previously by saturation analysis.

Saturation experiments using [^{125}I]AT-1012 were conducted in the presence of various concentrations of unlabeled epibatidine and using [^{3}H]epibatidine in the presence of unlabeled AT-1012 to determine the competitive or non-competitive nature of binding. Nonspecific binding was determined by using 1 μM of AT-1001 or 0.1 μM of unlabeled epibatidine.

In these experiments, incubations were carried out overnight (approximately 16 h) at 4° C to assure equilibrium of binding.

2.4. Brain Tissue Binding

Adult male Sprague-Dawley rats were decapitated after isoflurane anesthesia and the brains were quickly removed. The cerebellum was then collected and the rest of the brain put in a brain slicer (Zivic). Slices containing the MHb and IPN were obtained and those brain regions were crudely excised. The brain samples were then homogenized and binding was conducted essentially as described above.

2.5. In Vitro Autoradiography

Adult female Sprague-Dawley rats were decapitated after isoflurane anesthesia, and brains rapidly removed and frozen on dry ice. (Animal use and procedures were approved by the George Washington University Medical Center Institutional Animal Care and Use Committee.) Frozen sagittal brain sections (12 μm) were cut and mounted onto Superfrost Plus slides (Fisher Scientific, Newark, DE) and stored at −80°C until use. For autoradiography, [^{125}I]AT-1012 was added to Tris HCl buffer (50 mM, pH 7.4) at a concentration of 0.08 nM. Slides with frozen sections were allowed to reach room temperature, then incubated with 0.2–0.3 ml Tris buffer containing [^{125}I]AT-1012, with or without 300 μM unlabeled nicotine to yield non-specific binding. Following a 60 min incubation at room temperature, sections were rinsed in ice-cold buffer for 2 × 10 min, then rapidly air-dried. After overnight desiccation, sections were apposed to Kodak BioMax MR film for 4 days in a cold room. Film was developed in an automatic developer. Subsequent images were digitized using an MCID digital imaging system (InterFocus Imaging, Cambridge, UK).

3. Results

3.1. Receptor binding to α3β4 nAChR-transfected HEK cell membranes

[^{125}I]AT-1012 (Figure 1) binds with high affinity to α3β4 nAChR on membranes of HEK cells transfected with this receptor. As seen in Figure 2A, saturation analysis indicates a single binding site with a Bmax of 10.3 ± 1.67 pmol/mg protein and affinity of 1.40 ± 0.49 nM for [^{125}I]AT-1012. Because the high specific activity of the radioiodinated ligand (2200 Ci/mmol) precludes the ability to reach saturation, the [^{125}I]AT-1012 was diluted 10X with unlabeled AT-1012 prior to the saturation experiment. Under these conditions non-specific binding was still low. In contrast to the high affinity binding to the α3β4 nAChR-transfected HEK cell membranes, [^{125}I]AT-1012 exhibited no specific binding to α4β2 nAChR-containing HEK cell membranes (Figure 2B). This is consistent with the low binding affinity of AT-1012 and its other AT analogs for the α4β2 nAChR (see Table 1).

3.2. Binding characteristics of radioligand [^{125}I]AT-1012

Association and dissociation experiments were carried out to further characterize binding properties of [^{125}I]AT-1012 at the α3β4 nAChR. Both association and dissociation are rapid with half times of approximately 5 min each (Figure 3). When analyzed using Prism, both association and dissociation resulted in a best fit to a single phase with k_{on} and k_{off} values of 0.22 ± 0.11 nM^{-1} $minute^{-1}$ and 0.19 ± 0.05 $minute^{-1}$ respectively, resulting in a K_d calculated to be 0.86 nM. This value is consistent with the dissociation constant derived from the saturation experiment (Table 1).

3.3. Characterization of the [^{125}I]AT-1012 binding site

The pharmacological characteristics of the [^{125}I]AT-1012 binding site in α3β4 nAChR were determined in drug competition and saturation assays. As shown in Figure 4A, epibatidine inhibits [^{125}I]AT-1012 binding in an apparent not-strictly competitive manner. Due to the slow dissociation of the high affinity ligand epibatidine, these experiments were carried out

with a 16 h incubation. Increasing concentrations of epibatidine induced an increase in K_d and a slight decrease in the B_{max} of [^{125}I]AT-1012 binding to α3β4 nAChR (Figure 4A). Non-linear regression analysis of the saturation data resulted in K_d values of 0.22 nM, 0.34 nM and 1.04 nM and Bmax values of 7.92, 6.36, and 5.58 pmol/mg, for binding in the presence of 0, 0.5 nM and 1.5 nM epibatidine respectively.

The reciprocal experiment using [^{3}H]epibatidine as radioligand was also conducted with a 16 h incubation. Here, AT-1012 inhibition of [^{3}H]epibatidine binding also showed a decrease in K_d with a very small decrease in Bmax (Figure 4B). Non-linear regression analysis of the saturation data resulted in K_d values of 0.25 nM, 0.54 nM, 0.97 nM, and 2.84 nM; and Bmax values of 8.28 pmol/mg protein, 7.34 pmol/mg protein, 6.08 pmol/mg protein and 6.32 pmol/mg protein in the presence of 0, 5, 15, and 50 nM AT-1012, respectively.

These results are similar to what we observed with AT-1001, the α3β4 nAChR-selective ligand we reported previously (Toll *et al*., 2012). AT-1001 appeared to compete with [^{3}H]epibatidine binding in a manner not strictly competitive, and induced a decrease in both K_d and B_{max} in a [^{3}H]epibatidine saturation isotherm. However, the experiments with AT-1001 were done with 2 h incubation, and the slow dissociation of the high affinity ligand epibatidine likely resulted in non-equilibrium conditions, resulting in an apparent reduction in Bmax. Nevertheless, the extended incubation times in the current experiments still appeared to result in a non-competitive profile of binding. Whether this relatively small deviation for competitive inhibition is still a function of the experimental conditions is not completely clear.

A pharmacological evaluation of the binding site was conducted using [^{125}I]AT-1012 as the radioligand in competitive displacement assays with known ligands (Table 1). As expected, epibatidine, AT-1012, and AT-1001 show a very high affinity K_i for rat α3β4 nAChR, using [^{125}I]AT-1012 as a radioligand. The K_i observed for epibatidine is consistent with its K_d at the rat α3β4 nAChR (Table 1). Nicotine binds with the expected lower affinity, whereas mecamylamine and 18-MC do not inhibit [^{125}I]AT-1012 binding. The K_i values determined for the known ligands using [^{125}I]AT-1012 as the radioligand compare favorably with K_i values derived using [^{3}H]epibatidine as the radioligand, in the same membrane preparation (Table 1). As seen in Table 1, AT-1012, like AT-1001, has >100-fold lower binding affinity at the α4β2 nAChR than at the α3β4 nAChR (Toll *et al*., 2012).

We next determined whether [^{125}I]AT-1012 has similar high binding affinity to the human α3β4α5 nAChR subunit combination, expressed in HEK293 cells. As shown in Table 2, AT-1001 and AT-1012 had similar binding affinities at the human α3β4α5 nAChR, compared to the rat α3β4 nAChR, using [^{125}I]AT-1012 as the radioligand. As expected, 18-MC and mecamylamine do not compete with [^{125}I]AT-1012 at the human α3β4α5 nAChR.

[^{125}I]AT-1012 binding to a rat brain membrane preparation was also attempted, using a concentration of 0.03 nM of the radioligand. However, given the relatively low density of α3β4* nAChR in rat brain (Gotti *et al*., 2009), no specific binding could be measured in membranes from whole rat brain and cerebellum. Only very low specific binding could be detected from MHb obtained from a single rat, but this could not be quantified (data not shown).

3.2. In vitro autoradiography in rat brain slices with [^{125}I]AT-1012

Given the high selectivity of [^{125}I]AT-1012 for the α3β4 nAChR in binding studies, we investigated whether it could selectively visualize the small population of α3β4* nAChR in rat brain slices, using in vitro autoradiography. As seen in Figure 5, [^{125}I]AT-1012 heavily

labels the MHb, IPN, and fr, with lighter labeling detected in the granule layer of the cerebellum. Very heavy labeling was also detected in the pineal gland, a region expressing only the α3β4 subtype of nAChR (Figure 5C) (Perry *et al*., 2002). Several other regions have previously been reported to express much smaller amounts of α3β4* nAChR, including the inferior colliculus, hippocampus, anterior ventral nucleus of the thalamus, and several brainstem nuclei, notably area postrema (Marks *et al*., 2002; Perry *et al*., 2002). These areas were either not on the sections cut or there was not significant specific binding detected in these experiments. Notably, no specific binding of [^{125}I]AT-1012 was detected in areas such as cerebral cortex, known not to express α3β4* nAChRs. The α3β4* nAChR localization observed with [^{125}I]AT-1012 is consistent with previous autoradiographic studies for detecting the α3β4* nAChR subtype in the brain, which used the non-selective [^{3}H]epibatidine in the presence of a blocker of β2-containing nAChR, and the use of individual subunit null mutations, both of which yield a pattern of β4*-selective labeling (Baddick *et al*., 2011; Marks *et al*., 2002; Perry *et al*., 2002). Further, as seen in Figure 5, there is virtually no nonspecific binding of the radioligand in the tissue slices. These studies further confirm the selectivity of the radioligand [^{125}I]AT-1012, for the α3β4* nAChR in rat brain, and demonstrate its utility in labeling the limited but distinct localization of this nAChR population in the brain.

4. Discussion

nAChRs consist of a large family of ligand-gated ion channels that are involved in many CNS processes (Gotti *et al*., 1997; McGehee *et al*., 1995). The characterization of ligand binding to the acetylcholine binding site of the various subtypes has been accomplished with a variety of radioligands including [^{3}H]nicotine (Marks *et al*., 1982; Romano *et al*., 1980), [^{3}H]cytisine (Pabreza *et al*., 1991), and [^{3}H]epibatidine (Houghtling *et al*., 1995; Xiao *et al*., 2004) or its iodo analog [^{125}I]IPH (Davila-Garcia *et al*., 1997), among others. These ligands have been used to characterize the pharmacology and the location of the nAChR in the brain, using in vitro receptor binding studies and in vitro autoradiography respectively. Epibatidine binds with high affinity to all nAChRs and with particularly high affinity to α4β2* and α3β4* nAChRs (Badio *et al*., 1994; Gerzanich *et al*., 1995). However, because epibatidine binds with high affinity to both of these nAChR subtypes, it can only be used to label α3β4 nAChR after blocking its binding to α4β2 nAChR with ligands that selectively bind α4β2 nAChR, such as 5 nM of the β2-subunit selective compound A-85380, or using β2 KO mice (Baddick *et al*., 2011; Marks *et al*., 2002; Perry *et al*., 2002). Using such techniques, it was determined that the greatest brain concentration of α3β4* nAChR is in the MHb-IPN pathway.

[^{125}I]AT-1012 appears to be an excellent ligand to selectively radiolabel α3β4* nAChR. In the competitive binding experiments shown in Fig. 2B, [^{125}I]AT-1012 shows very high specific binding to HEK cell membranes expressing α3 β4 nAChR, Binding affinities determined with [^{125}I]AT-1012 are consistent and comparable with binding affinities determined using [^{3}H]epibatidine (Table 1). Our data show that [^{125}I]AT-1012 does not bind to α4β2 or α7 nAChR , but has equally high affinity for the human α3β4α5 nAChR subtype (Table 2). We are currently acquiring transfected cells with additional nAChR subtypes to better characterize its nAChR selectivity and binding profile.

[^{125}I]AT-1012 appears to bind to a single site on the α3β4* nAChR, as determined by both saturation and kinetic analysis (Figure 2 and 3). The binding interaction between epibatidine and AT-1012 or AT-1001 is not completely clear. Saturation experiments with [^{125}I]AT-1012 in the presence of various concentrations of unlabeled epibatidine, or the reciprocal experiment with [^{3}H]epibatidine and unlabeled AT-1012, showed changes in K_d with a small decrease in Bmax. The experimental protocol plays an important role in the

outcome of this experiment. For normal binding experiments, a 2 h incubation protocol is typically used. However, the affinity of epibatidine is very high and dissociation very slow. When these saturation experiments were initially conducted for 2 h, we found a decrease in B_{max} with no apparent change in K_d, suggesting a non-competitive binding profile with respect to epibatidine (data not shown). A slow dissociation of epibatidine could result in an apparent non-competitive interaction in the saturation experiments, if binding is not at equilibrium. In the experiments reported here, a 16 h incubation was used, to allow equilibrium to occur. However, these experiments still result in a small decrease in Bmax with an increase in the dissociation constant, suggesting a mixed type of inhibition.

The usefulness of this radioligand is not merely in binding to membranes from transfected cells, as [^{3}H]epibatidine can easily be used for that purpose. With the high specific activity and longer decay times of the ^{125}I radiolabel, and the high binding affinity and selectivity for the α3β4* nAChR subtype, [^{125}I]AT-1012 is more useful for selective labeling of the α3β4* nAChR subtype and in autoradiography experiments conducted on brain or peripheral tissues that contain more than a single nAChR subtype. As reported here (Figure 5), the in vitro autoradiographic experiments in rat brain slices show very dense binding specifically in regions known to have high concentrations of α3β4* nAChR, whereas no specific binding was observed in areas known not to express the α3β4 receptors. [^{125}I]AT-1012 binding is seen in the MHb, IPN, the fasciculus retroflexus, and the pineal gland (Figure 5), along with granular layer of the cerebellum. This localization of α3β4* nAChR is consistent with that seen with [^{125}I]IPH binding in the presence of 5 nM A-85380, as described by Perry et al. (Perry *et al*., 2002). However, we did not detect specific binding in hippocampus nor inferior colliculus, regions previously shown to contain α3β4* receptors. It is possible that the amount of the α3β4* nAChR population in these regions are below the level of detection or that the α3β4* nAChR subpopulation in these regions may contain other accessory subunits, which may have altered affinity for the AT-1012-type α3β4 ligands.

The true selectivity of this class of compounds is not yet completely understood. [^{125}I]AT-1012 binds with high affinity to α3β4, but not α3β4 nAChR. The presence of an accessory subunit, such as α5, as in the α3β4α5 nAChR subtype tested here, does not appear to influence binding to a great degree, since both [^{125}I]AT-1012 and [^{3}H]epibatidine binding appears to be quite similar in rat α 3β4 and human α3β4α5 cell lines. In the autoradiographic experiments, it appears that [^{125}I]AT-1012 labels both the MHb and the IPN with equal and high density. It has been previously shown that by Grady et al. (2009) that the predominant subpopulation of the α3β4* nAChR in the rat MHb and IPN is the β3-containing α3β4β3* nAChR. The α5-containing α3β4* nAChR subpopulation, on the other hand, is predominantly found in the peripheral ganglia, and is present to a much lesser extent in the MHb and IPN (Gotti *et al*., 2009). The high labeling of both the MHb and the IPN by [^{125}I]AT-1012 suggests that it has high binding affinity for the α3β4β3 subpopulation of the α3β4* nAChR, predominant in rat brain.

In summary, [^{125}I]AT-1012 is a high affinity and selective radioligand that could be a very useful tool to label the α3β4* nAChR. Given its high binding affinity and binding selectivity for the α3β4* nAChR and the high specific activity of the radiolabel, [^{125}I]AT-1012 is not only suitable for receptor binding studies using cell membrane homogenates but can also be used for localization of the limited populations of the α3β4* nAChR in brain by autoradiography. AT-1012 belongs to the same series of high affinity and selective nAChR antagonists as AT-1001, which we showed, blocks nicotine self-administration in rats when given systemically (Toll *et al*., 2012). Because of the potential importance of the α3β4* nAChR in reward induced by nicotine and other abused drugs, a selective small-molecule ligand such as [^{125}I]AT-1012 should be an excellent tool to study the role of the α3β4* nAChR in nicotine addiction and the reward process in general.

Acknowledgments

This work was supported by the National Institutes of Health's National Institute on Drug Abuse Grants R01DA020811 and R43DA033744. Support for L.T. and J.W. by the State of Florida, Executive Office of the Governor's Office of Tourism, Trade, and Economic Development, is also gratefully acknowledged.

References

Baddick CG, Marks MJ. An autoradiographic survey of mouse brain nicotinic acetylcholine receptors defined by null mutants. Biochem Pharmacol. 2011; 82(8):828–841. [PubMed: 21575611]

Badio B, Daly JW. Epibatidine, a potent analgetic and nicotinic agonist. Mol Pharmacol. 1994; 45(4): 563–569. [PubMed: 8183234]

Berrettini W, Yuan X, Tozzi F, Song K, Francks C, Chilcoat H, Waterworth D, Muglia P, Mooser V. Alpha-5/alpha-3 nicotinic receptor subunit alleles increase risk for heavy smoking. Mol Psychiatry. 2008; 13(4):368–373. [PubMed: 18227835]

Cheng Y, Prusoff WH. Relationship between the inhibition constant (K1) and the concentration of inhibitor which causes 50 per cent inhibition (I50) of an enzymatic reaction. Biochem Pharmacol. 1973; 22(23):3099–3108. [PubMed: 4202581]

Davila-Garcia MI, Musachio JL, Perry DC, Xiao Y, Horti A, London ED, Dannals RF, Kellar KJ. [125I]IPH, an epibatidine analog, binds with high affinity to neuronal nicotinic cholinergic receptors. J Pharmacol Exp Ther. 1997; 282(1):445–451. [PubMed: 9223586]

Gerzanich V, Peng X, Wang F, Wells G, Anand R, Fletcher S, Lindstrom J. Comparative pharmacology of epibatidine: a potent agonist for neuronal nicotinic acetylcholine receptors. Mol Pharmacol. 1995; 48(4):774–782. [PubMed: 7476906]

Glick SD, Maisonneuve IM. Development of novel medications for drug addiction. The legacy of an African shrub. Ann N Y Acad Sci. 2000a; 909:88–103. [PubMed: 10911925]

Glick SD, Maisonneuve IM, Dickinson HA. 18-MC reduces methamphetamine and nicotine self-administration in rats. Neuroreport. 2000b; 11(9):2013–2015. [PubMed: 10884062]

Glick SD, Maisonneuve IM, Kitchen BA. Modulation of nicotine self-administration in rats by combination therapy with agents blocking alpha 3 beta 4 nicotinic receptors. Eur J Pharmacol. 2002; 448(2–3):185–191. [PubMed: 12144940]

Glick SD, Maisonneuve IM, Szumlinski KK. 18-Methoxycoronaridine (18-MC) and ibogaine: comparison of antiaddictive efficacy, toxicity, and mechanisms of action. Ann N Y Acad Sci. 2000c; 914:369–386. [PubMed: 11085336]

Glick SD, Ramirez RL, Livi JM, Maisonneuve IM. 18-Methoxycoronaridine acts in the medial habenula and/or interpeduncular nucleus to decrease morphine self-administration in rats. Eur J Pharmacol. 2006; 537(1–3):94–98. [PubMed: 16626688]

Gotti C, Clementi F, Fornari A, Gaimarri A, Guiducci S, Manfredi I, Moretti M, Pedrazzi P, Pucci L, Zoli M. Structural and functional diversity of native brain neuronal nicotinic receptors. Biochem Pharmacol. 2009; 78(7):703–711. [PubMed: 19481063]

Gotti C, Fornasari D, Clementi F. Human neuronal nicotinic receptors. Prog Neurobiol. 1997; 53(2): 199–237. [PubMed: 9364611]

Grady SR, Meinerz NM, Cao J, Reynolds AM, Picciotto MR, Changeux JP, McIntosh JM, Marks MJ, Collins AC. Nicotinic agonists stimulate acetylcholine release from mouse interpeduncular nucleus: a function mediated by a different nAChR than dopamine release from striatum. J Neurochem. 2001; 76(1):258–268. [PubMed: 11145999]

Grady SR, Moretti M, Zoli M, Marks MJ, Zanardi A, Pucci L, Clementi F, Gotti C. Rodent habenulo-interpeduncular pathway expresses a large variety of uncommon nAChR subtypes, but only the alpha3beta4* and alpha3beta3beta4* subtypes mediate acetylcholine release. J Neurosci. 2009; 29(7):2272–2282. [PubMed: 19228980]

Houghtling RA, Davila-Garcia MI, Kellar KJ. Characterization of (+/−)(−)[3H]epibatidine binding to nicotinic cholinergic receptors in rat and human brain. Mol Pharmacol. 1995; 48(2):280–287. [PubMed: 7651361]

Jiang F, Bupp J, Rhee S, Toll L, Zaveri NT. Radiosynthesis of a 125I analog of a highly selective alpha3beta4 nicotinic acetylcholine receptor antagonist ligand for use in autoradiography studies. Journal of Labelled Compounds and Radiopharmaceuticals. 2012; 55(5):177–179.

Luo S, Kulak JM, Cartier GE, Jacobsen RB, Yoshikami D, Olivera BM, McIntosh JM. alpha-conotoxin AuIB selectively blocks alpha3 beta4 nicotinic acetylcholine receptors and nicotine-evoked norepinephrine release. J Neurosci. 1998; 18(21):8571–8579. [PubMed: 9786965]

Maisonneuve IM, Glick SD. Anti-addictive actions of an iboga alkaloid congener: a novel mechanism for a novel treatment. Pharmacol Biochem Behav. 2003; 75(3):607–618. [PubMed: 12895678]

Marks MJ, Collins AC. Characterization of nicotine binding in mouse brain and comparison with the binding of alpha-bungarotoxin and quinuclidinyl benzilate. Mol Pharmacol. 1982; 22(3):554–564. [PubMed: 7155123]

Marks MJ, Whiteaker P, Grady SR, Picciotto MR, McIntosh JM, Collins AC. Characterization of [(125) I]epibatidine binding and nicotinic agonist-mediated (86) Rb(+) efflux in interpeduncular nucleus and inferior colliculus of beta2 null mutant mice. J Neurochem. 2002; 81(5):1102–1115. [PubMed: 12065623]

McCallum SE, Cowe MA, Lewis SW, Glick SD. alpha3beta4 nicotinic acetylcholine receptors in the medial habenula modulate the mesolimbic dopaminergic response to acute nicotine in vivo. Neuropharmacology. 2012; 63(3):434–440. [PubMed: 22561751]

McCallum SE, Glick SD. 18-Methoxycoronaridine blocks acquisition but enhances reinstatement of a cocaine place preference. Neurosci Lett. 2009; 458(2):57–59. [PubMed: 19442876]

McGehee DS, Heath MJ, Gelber S, Devay P, Role LW. Nicotine enhancement of fast excitatory synaptic transmission in CNS by presynaptic receptors. Science. 1995; 269(5231):1692–1696. [PubMed: 7569895]

Pabreza LA, Dhawan S, Kellar KJ. [3H]cytisine binding to nicotinic cholinergic receptors in brain. Mol Pharmacol. 1991; 39(1):9–12. [PubMed: 1987453]

Perry DC, Xiao Y, Nguyen HN, Musachio JL, Davila-Garcia MI, Kellar KJ. Measuring nicotinic receptors with characteristics of alpha4beta2, alpha3beta2 and alpha3beta4 subtypes in rat tissues by autoradiography. J Neurochem. 2002; 82(3):468–481. [PubMed: 12153472]

Rezvani AH, Overstreet DH, Yang Y, Maisonneuve IM, Bandarage UK, Kuehne ME, Glick SD. Attenuation of alcohol consumption by a novel nontoxic ibogaine analogue (18-methoxycoronaridine) in alcohol-preferring rats. Pharmacol Biochem Behav. 1997; 58(2):615–619. [PubMed: 9300627]

Romano C, Goldstein A. Stereospecific nicotine receptors on rat brain membranes. Science. 1980; 210(4470):647–650. [PubMed: 7433991]

Saccone SF, Saccone NL, Swan GE, Madden PA, Goate AM, Rice JP, Bierut LJ. Systematic biological prioritization after a genome-wide association study: an application to nicotine dependence. Bioinformatics. 2008; 24(16):1805–1811. [PubMed: 18565990]

Salas R, Pieri F, De Biasi M. Decreased signs of nicotine withdrawal in mice null for the beta4 nicotinic acetylcholine receptor subunit. J Neurosci. 2004; 24(45):10035–10039. [PubMed: 15537871]

Toll L, Zaveri NT, Polgar WE, Jiang F, Khroyan TV, Zhou W, Xie XS, Stauber GB, Costello MR, Leslie FM. AT-1001: A High Affinity and Selective alpha3beta4 Nicotinic Acetylcholine Receptor Antagonist Blocks Nicotine Self-Administration in Rats. Neuropsychopharmacology. 2012

Xiao Y, Kellar KJ. The comparative pharmacology and up-regulation of rat neuronal nicotinic receptor subtype binding sites stably expressed in transfected mammalian cells. J Pharmacol Exp Ther. 2004; 310(1):98–107. [PubMed: 15016836]

Highlights

- [^{125}I]AT-1012 binds with high affinity to α3β4 nAChR in transfected cells
- [^{125}I]AT-1012 binds with equally high affinity to human α3β4α5 nAChR in transfected cells
- Using [^{125}I]AT-1012, in vitro autoradiography can visualize α3β4* nAChR in rat brain
- [^{125}I]AT-1012 does not label β2-containing nAChR
- [^{125}I]AT-1012 is a new tool to selectively label α3β4* nAChR

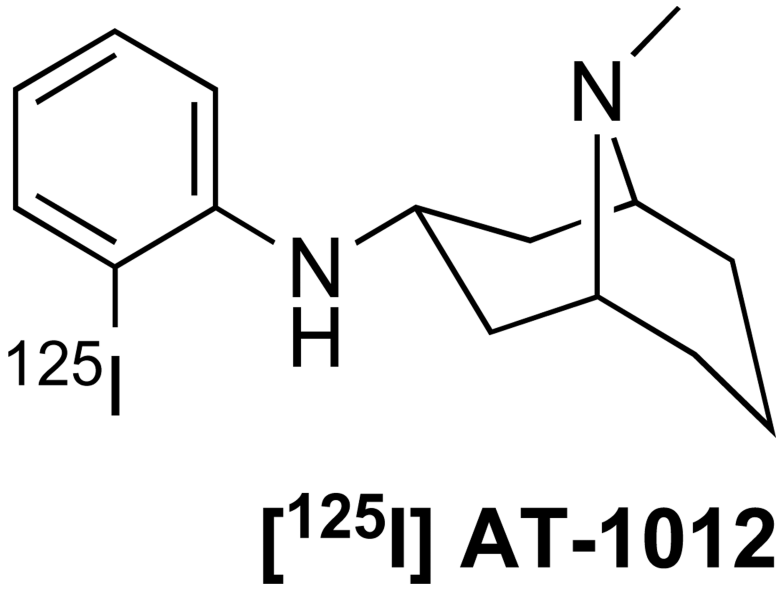

Figure 1.
Structure of [^{125}I]AT-1012

A

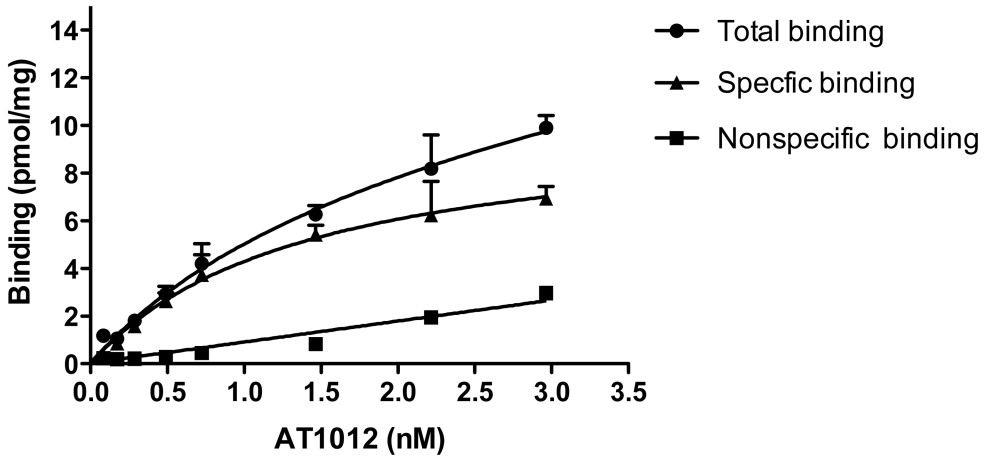

B

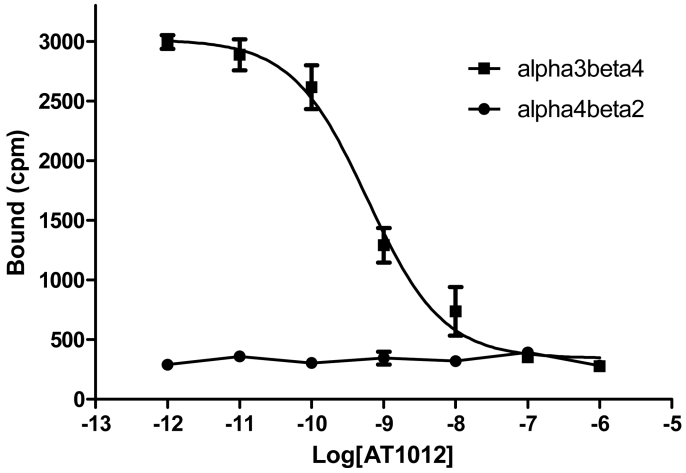

Figure 2.

(***A***). Saturation isotherm for [^{125}I]AT-1012. This curve was derived from an experiment in which the [^{125}I]AT-1012 was diluted 10X with unlabeled AT-1012 so that increasing radioactivity would result in concentrations above and below the K_d. In this experiment, concentrations ranged from 0.1 to 3.0 nM. This experiment was repeated twice with similar results. (***B***). [^{125}I]AT-1012 selectively binds to α3β4 nAChR. Binding was conducted as described in Materials and Methods. The cell membranes containing α3β4 nAChR or α4β2 nAChR were incubated with 10^{-6} to 10^{-12} M unlabeled AT-1012 in the presence of 0.03 nM [^{125}I]AT-1012 for 2 hours. The cell membranes were filtered using a Tomtec cell

harvester and were counted on a betaplate reader (Wallac). Data show average ± SD from one representative experiment conducted in triplicate for [^{125}I]AT-1012 binding.

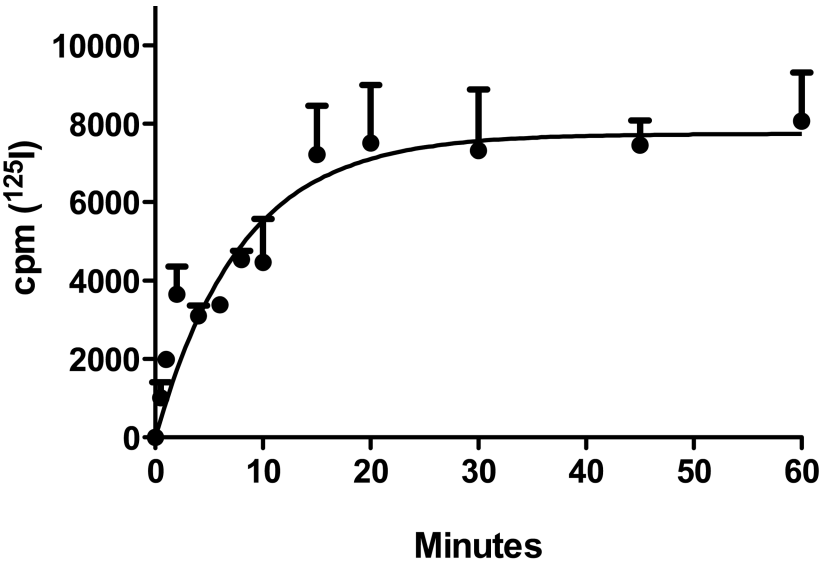

A

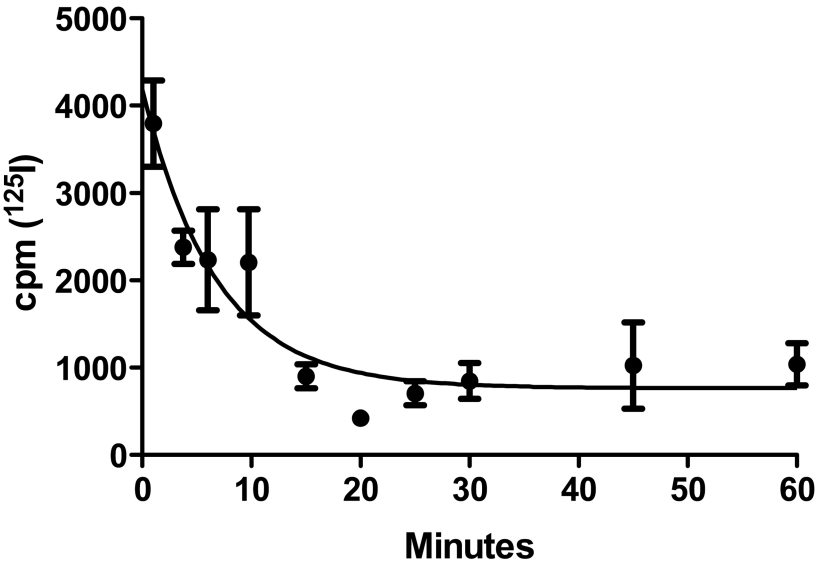

B

Figure 3. Kinetics of [^{125}I]AT-1012 binding

[^{125}I]AT-1012 binding was conducted as described in Materials and Methods. (***A)***. For association experiments, [^{125}I]AT-1012 was incubated with the cellular membrane containing α3β4 nAChR at indicated time points and nonspecific binding was measured at the time points using unlabeled AT-1012 (1 μM) as blank. (***B)***. For the dissociation experiments, after incubation to equilibrium (1 h), dissociation was initiated by addition of excess unlabeled AT-1012 (1 μM) to each well at appropriate times so that upon filtration it resulted in dissociation times displayed in the figure. The figure shows data from single experiments conducted in quadruplicate that were repeated with similar results. In the

experiments shown, k_{on} and k_{off} values were 0.13 $nM^{-1}min^{-1}$ and 0.15 min^{-1} respectively. The values shown in the Results section represent the averages derived from the two experiments.

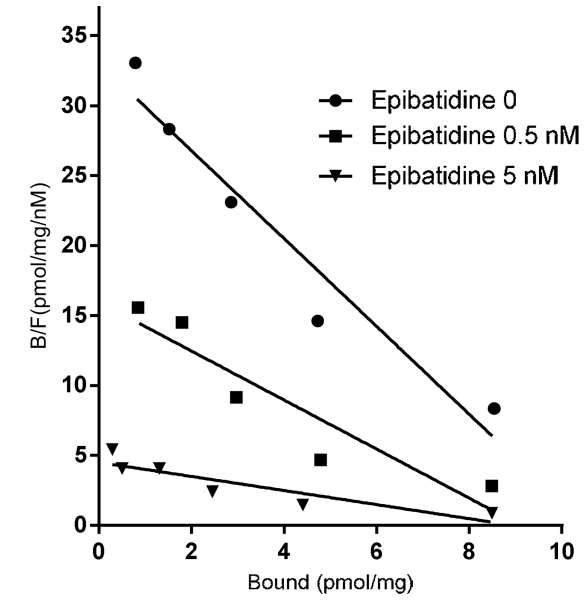

A

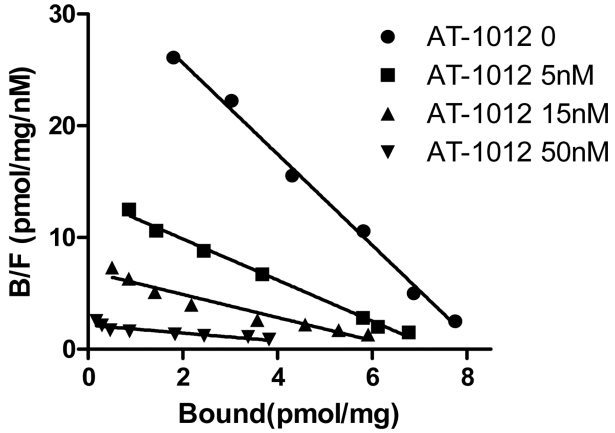

B

Figure 4.

(***A)*** **Inhibition of [^{125}I]AT-1012 saturation with epibatidine**. [^{125}I]AT-1012 saturation experiments were conducted in the presence of 0, 0.5 nM and 1.5 nM epibatidine to examine the competitive or non-competitive nature of binding. Non-linear regression analysis of the saturation data resulted in K_d values of 0.22 nM, 0.34 nM and 1.04 nM; and Bmax values of 7.92, 6.36, and 5.58 pmol/mg, for binding in the presence of 0, 0.5 nM and 1.5 nM epibatidine respectively. Nonspecific binding was determined using 0.1 μM of unlabeled epibatidine. (***B)***. **Inhibition of [^{3}H]epibatidine saturation with AT-1012**. [^{3}H]Epibatidine saturation experiments were conducted in the presence of 0, 5 nM, 15 nM, and 50 nM

AT-1012 in triplicate. Non-linear regression analysis of the saturation data resulted in K_d values of 0.25 nM, 0.54 nM, 0.97 nM, and 2.84 nM; and Bmax values of 8.28 pmol/mg protein, 7.34 pmol/mg protein, and 6.08 pmol/mg protein; and 6.32 pmol/mg protein for Scatchard analysis in the presence of 0, 5, 15, and 50 nM AT-1001, respectively. Nonspecific binding was determined by using 1 μM of AT-1012 of unlabeled epibatidine.

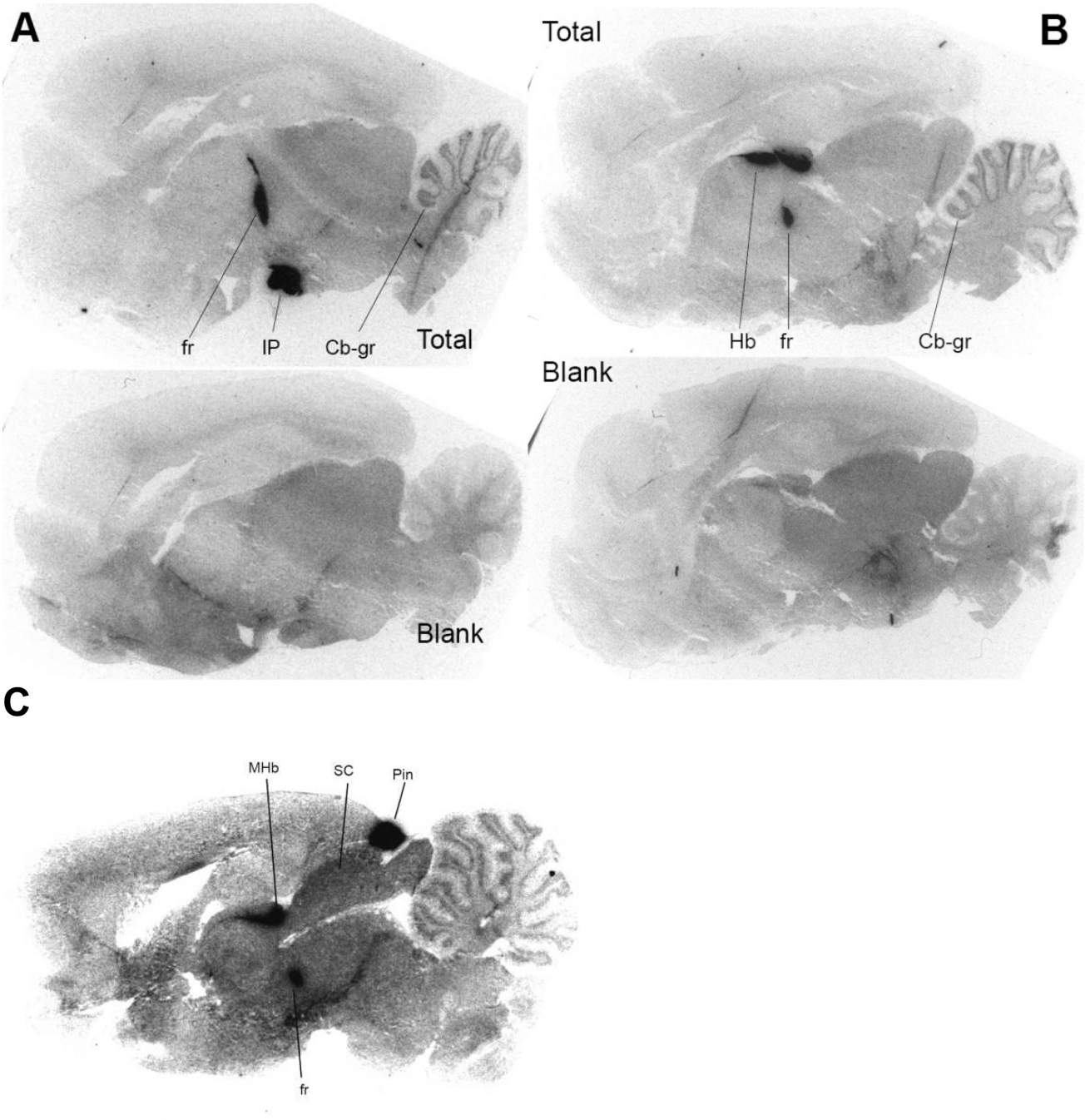

Figure 5. In vitro autoradiographic localization of [^{125}I]AT-1012 binding

Binding is shown in two sagittal sections, A and B; top images represent total binding, while bottom images represent non-specific binding of [^{125}I]AT-1012 in the presence of 300 μM nicotine in sections adjacent to the corresponding total binding. Panel C shows total binding including the pineal gland, Pin; Cb-gr, cerebellar granule layer; fr, fasciculus retroflexus; Hb, habenula; IP, interpenduncular nucleus.

Table 1

Binding affinity of selected compounds at the rat α3β4 nAChR using [^{125}I]AT-1012 and the rat α3β4 and α3β4 nAChR using [^{3}H]epibatidine

Binding was conducted as described in Materials and Methods. Data show average ± SD from at least 2 experiments conducted in triplicate for [^{3}H]epibatidine binding and quadruplicate for [^{125}I]AT-1012 binding. In each cell, the upper line is the K_i and the lower line, in parentheses, is the Hill coefficient. [^{125}I]AT-1012 does not have specific binding to α3β4 nAChR.

	Binding affinity (K_i nM)		
	[^{125}I]AT-1012	[^{3}H]epibatidine	
Compound	**α3β4 nAChR**	**α3β4 nAChR**	**α4β2 nAChR**
Epibatidine	0.44 ± 0.04 *(0.89± 0.01)*	0.62±0.03 *(1.00± 0.06)*	0.27±0.08 *(1.05± 0.05)*
Nicotine	467±48 *(0.68± 0.02)*	666±106 *(1.08± 0.12)*	47.80±4.24 *(0.95± 0.07)*
18-MC	> 10,000	> 10,000	> 10,000
Mecamylamine	> 10,000	> 10,000	> 10,000
AT-1001	0.65 ± 0.14 *(0.94± 0.04)*	1.96 ± 0.13 *(0.87± 0.19)*	263 ± 9.3 *(0.97± 0.11)*
AT-1012	0.40 ± 0.02 *(1.03± 0.01)*	1.30 ± 0.16 *(0.77± 0.09)*	142 ± 2.0 *(0.88± 0.02)*

Table 2

Binding affinity of selected compounds at the human α3β4α5 nAChR using [^{125}I]AT-1012 and [^{3}H]epibatidine as radioligands

Binding was conducted as described in Materials and Methods. Data show average ± SD from at least 2 experiments conducted in triplicate for [^{3}H]epibatidine binding and quadruplicate for [^{125}I]AT-1012 binding. In each cell, the upper line is the K_i and the lower line, in parentheses, is the Hill coefficient. [^{125}I]AT-1012 does not have specific binding to α4β2 nAChR.

Binding affinity (K_i nM) at human α3β4α5 nAChR		
Compound	**[^{125}I]AT-1012**	**[^{3}H] epibatidine**
Epibatidine	1.10±0.04 *(0.88± 0.02)*	0.58±0.02 *(0.98± 0.02)*
Nicotine	1305±219 *(0.75± 0.05)*	1573±35 *(0.91± 0.04)*
AT-1001	1.75±0.14 *(0.95± 0.05)*	3.34±0.03 *(0.82± 0.04)*
AT-1012	0.68±0.06 *(0.96± 0.09)*	1.08±0.05 *(0.81 ± 0.0 3)*